

# Characterization of a CMOS Geiger Photodiode Pixel

Christopher J. Stapels, *Member, IEEE*, William G. Lawrence, Frank L. Augustine, *Member, IEEE*, and James F. Christian, *Member, IEEE*

**Abstract**—This paper examines the performance of CMOS avalanche photodiode pixels operated in a Geiger mode. The pixels, called Geiger photodiode (GPD) pixels, convert an incident analog photon flux into a digital count rate. The maximum detection efficiency of the characterized GPD pixel for 632-nm light is 22%. The passively quenched GPD pixel exhibits an after pulsing at excess bias voltages above 2 V, and a minimum in the after-pulsing correction factor, of 0.53, occurs at an excess bias of 5.8 V. The after pulsing increases the fluctuations, or noise, in the count-rate signal. The following expression accurately describes the noise in the characterized GPD pixel, which exhibits a relatively low after-pulsing probability:  $\sigma^2 = \bar{n}_{dp} + \bar{n}_{ap} + 2 \cdot [\bar{n}_{dp} \cdot \bar{n}_{ap}]^{1/2}$ , where  $\sigma$  represents the count-rate fluctuations, the “dp” subscript stands for “detected photons,” the “ap” subscript stands for “after pulses,” and the  $\bar{n}$  represents the “average count rate of” dp, or ap. The noise-equivalent illumination exhibits a minimum of 300 Hz at an operating voltage of 28 V. The best operating voltage for the GPD pixel increases from 28 V with increasing signal intensity.

**Index Terms**—Avalanche photodiode (APD), Geiger photodiode (GPD), noise measurement, semiconductor device noise.

## I. INTRODUCTION

IN RECENT years, CMOS active pixel sensor (APS) cameras have emerged as a promising alternative to charge-coupled device (CCD) cameras for certain specific medical applications, such as an intraocular vision aid [1], because the CMOS environment facilitates the integration of signal processing electronics. Significant progress has been made in reducing the readout noise and improving the performance of CMOS APS cameras [2]–[4]. Most current designs, however, store the integrated signal at each pixel location as an amount of charge, which is proportional to the photocurrent. The use of pixels that can internally amplify the signal to improve the signal-to-noise characteristics represents an evolutionary step forward in CMOS imaging technology.

Avalanche photodiode (APD) pixels are devices that can provide an internal gain with high-bandwidth characteristics. When used as proportional detectors, the APD functions as a photodiode that multiplies the incident photocurrent as the charge propagates through the device, thereby producing gain. The reverse bias increases and extends the internal-electric

Manuscript received September 20, 2005; revised January 16, 2006. This work was supported in part by the National Aeronautics and Space Administration (NASA) under Contract NNG04CA26C. The review of this paper was arranged by Editor J. Hynecek.

C. J. Stapels, W. G. Lawrence, and J. F. Christian are with Radiation Monitoring Devices, Inc., Watertown, MA 02472 USA (e-mail: JChristian@RCN.com).

F. L. Augustine is with Augustine Engineering, Encinitas, CA 92024 USA (e-mail: S.Augustine@IEEE.org).

Digital Object Identifier 10.1109/TED.2006.871170

field created by the migration of charge at the p-n junction in the depletion region. This internal-electric field accelerates the photocurrent and enables its multiplication through an impact ionization. In proportional mode, APDs are good for the high-gain high-bandwidth amplification of optical signals.

APDs can be operated in a separate mode, called the Geiger mode, to enable a single optical-photon sensitivity with sub-nanosecond timing characteristics [5]–[10]. In Geiger mode, the APD is biased above its breakdown voltage (BV), and a single photoelectron initiates a self-propagating avalanche caused by the iterative multiplication of both the electrons and holes at high internal-electric-field strengths [10]. This phenomenon is known as an avalanche breakdown. Unchecked, this self-propagating avalanche would cause the diode to conduct enough current to overheat. If, however, a circuit element detects the presence of this avalanche current, and subsequently drops the bias below the BV, the self-propagating avalanche will be quenched. After quenching, the bias can then be raised again, above breakdown, awaiting the arrival of another single-photoelectron event, thereby resetting the Geiger APD pixel. Used in this Geiger mode, the APD pixels, called Geiger photodiode (GPD) pixels, are capable of counting individual optical photons.

The detection of photons by an array of Geiger APD pixels represents a true all-digital single photon-counting imaging technology because the pixels produce the digital pulses for each photon detected. This digital, photon-counting approach eliminates the readout noise associated with an analog, or a proportional, detection. In imaging applications, the CMOS APD Geiger pixel enables the use of digital-counter flip/flops to store the signal at each pixel location. The future development of the associated digital components in a CMOS environment represents a benefit of CMOS APD pixel technology. In essence, the CMOS GPD camera represents a next-generation of CMOS APS cameras, where the photo-MOS pixels, or photodiode pixels are replaced with the GPD pixels.

Other efforts have developed CMOS, or CMOS compatible GPD pixels for photon-counting imaging arrays. Jackson *et al.* have thoroughly analyzed the optical crosstalk between the pixels in their arrays and have compared the radiometric performance of their GPD pixels to other available detectors [11]. Besse *et al.* use an industrial CMOS process to fabricate their pixels, and they have quantified the after pulsing in their actively quenched GPD pixels [12]. The design of the pixel presented in this paper is similar to that described by Besse *et al.*, and is referred to as “design 12” in this paper. Fig. 1 illustrates a cross-sectional view of the “design 12” pixel.

The Geiger junction in the GPD pixel illustrated in Fig. 1 is isolated from the p-substrate. The p-tub structure prevents

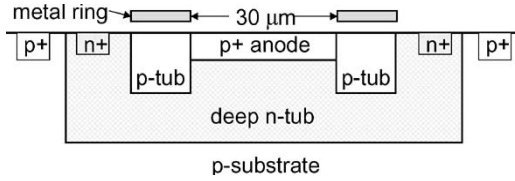


Fig. 1. Cross-sectional illustration of the “design 12” pixel. The p-tub structure prevents breakdown at the edge of the 30- $\mu\text{m}$  diameter photodiode pixel when it is operated in Geiger mode. In Geiger mode, the diode junction between the p+ anode and the deep n-tub is biased above the reverse bias BV. The structures in the illustration are not drawn to scale.

breakdown at the edge of the 30- $\mu\text{m}$  diameter photodiode pixel when it is operated in Geiger mode. The GPD pixel characterized in this paper is part of an array of test pixels fabricated with an existing commercial CMOS process.

This article presents the characterization of the a single optical-photon detection efficiency (DE), the after-pulsing noise, the noise-equivalent illumination (NEI), and the best operating voltage (BOV) for a passively quenched Geiger APD pixel as a function of the excess bias. The DE represents the efficiency in creating a Geiger pulse when a single optical-photon impinges on the detector. It is the product of the quantum efficiency (QE) and a bias-dependent Geiger probability. The after pulsing refers to the number of Geiger pulses produced by a single optical-photon Geiger event. The delayed release of charge by traps in the device produces delayed Geiger pulses, referred to as after pulses, which is correlated to the initiating Geiger event.

## II. EXPERIMENTAL METHODS

The purpose of the experiment is to measure the DE of a GPD pixel, quantify the after pulsing, and measure the noise, or count-rate fluctuations. The difference between the “LED on” and “LED off” count rate gives the LED light signal. The LED light signal divided by the calibrated photodiode response gives the “apparent DE.” This “apparent DE” includes after pulses. The amount of the GPD after pulsing is quantified using a pulsed laser-diode source. The diode laser source has a temporal width of  $< 3$  ns, a repetition rate of 4.1 kHz, and produces  $\sim 600$  photons per pulse over the active area of the GPD pixel. The laser-diode intensity is sufficient to insure that each pulse produces a Geiger event. The measured increase in the count rate is greater than the 4.1 kHz from the laser-diode source. These additional counts are attributed to the after pulsing.

632-nm light, from a bank of LEDs, uniformly illuminates the 30- $\mu\text{m}$  diameter GPD pixel (AE183, chip 8, pin-9 anode, pin-10 cathode) and a Thor Labs photodiode (DET 210). The passively quenched GPD pixel, connected to a Tektronix active probe (P6202) through a 3-nF capacitor, produces a Geiger pulse for each detected photoelectron. A timing-filter amplifier (Canberra 2111) differentiates the signal from the active probe, with a 100-ns time constant, and amplifies the Geiger pulses. The external trigger input of pulse generator (Tektronix PG508) discriminates the Geiger pulses from the baseline noise. A universal counter counts the pulses generated by the triggered

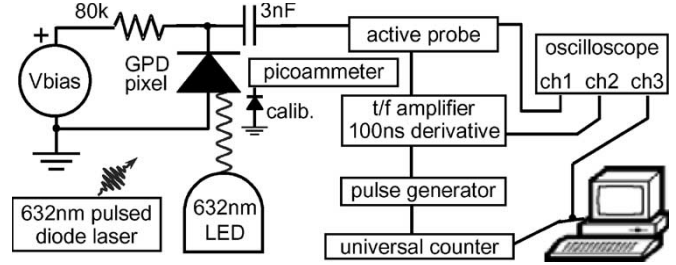


Fig. 2. Illustration of the measurement setup. The photosignal from the passively quenched 30- $\mu\text{m}$  diameter GPD pixel is amplified and differentiated by a timing-filter amplifier, denoted as “t/f amplifier” in the figure. The gain of the amplifier is adjusted to maintain constant amplitude for the average signal that triggers the pulse generator. The Geiger pulses are counted by a universal counter.

pulse generator and transmits the 1-s count-rate samples to a personal computer. The integration time for the measured count rates, the dark count rate (DCR) and the illuminated count rate (ICR), is 1 s. The standard deviation of forty 1-s samples, or readings, quantifies the count-rate fluctuations. Fig. 2 illustrates the experimental setup.

In characterizing the performance of the CMOS APD pixels in Geiger mode, we passively quench the devices with an  $\sim 80\text{-k}\Omega$  current-limiting resistor, which quenches the Geiger event by lowering voltage across the APD, below the BV, when a Geiger event occurs. When passively quenched, the amplitude of the Geiger pulse depends on the excess bias, or the amount of bias applied to the GPD in excess of its reverse-bias BV. The GPD pixel is biased by applying a positive voltage to the cathode of the GPD, while the anode, substrate, and chip carrier are grounded. Geiger pulses are generally uniform in their distribution of pulse heights, however, when a second event occurs during the recharge time of the pixel, which is  $\sim 5$   $\mu\text{s}$ , the amplitude of the second pulse will be less than the excess bias. For the measurements at different operating voltages, the average differentiated amplitude of the Geiger pulses, which trigger the pulse generator, is a constant value of 3 V, obtained by adjusting the gain of the timing-filter amplifier. Therefore, the trigger threshold of the pulse generator can be fixed at  $\sim 50$  mV to count the Geiger pulses from measurements at different operating voltages.

The DE and the room-temperature DCR represent important characteristics of the GPD pixel. The thermal generation of electron-hole pairs create Geiger pulses referred to as “dark counts.” The incident-photon flux is measured by uniformly illuminating the test pixel and a Thor Labs photodiode (model DET 210) pixel, which was calibrated against a Hamamatsu S1336-8BQ photodiode, and is connected to a picoammeter (Keithley 485). Moving the Thorlabs photodiode through the illumination area and observing a variation of less than 5% confirmed the uniformity of the illumination.

## III. RESULTS

This experiment measures the count rate as a function of an operating voltage in the presence and absence of an incident-photon signal. The after-pulsing correction factor at a given applied bias, calculated from the count rate of the laser signal,

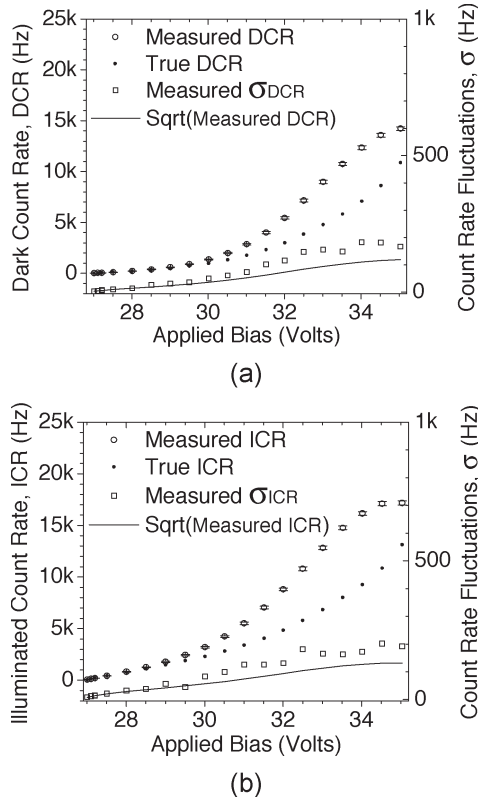


Fig. 3. (a) DCR as a function of the operating voltage. The left axis applied to the raw DCR, the measured DCR, and the DCR corrected for after pulsing, the true DCR. The right axis provides the scale for the measured dark count-rate fluctuations, and the estimated Schottky-noise fluctuations from the square root of the DCR. (b) ICR as a function of the operating voltage. This represents the count rate measured when the LED illuminates the GPD pixel and includes the contribution from the DCR.

applies to both the DCR and the ICR. Fig. 3(a) plots the measured DCR as a function of the operating voltage at a room temperature.

As can be seen in the figure, the DCR increases with the applied bias. The figure also shows the DCR after correcting for the after pulsing, labeled “True DCR,” which applies the correction for the after pulsing determined with the pulsed diode laser to the DCR. This correction to the DCR assumes that the amount of after pulsing depends on the bias, and not the signal source, e.g., thermal, LED, or laser diode. The amount of after pulsing in the DCR increases as the applied bias exceeds 30 V. The square root of the measured DCR estimates the Schottky-noise contribution. The difference between the Schottky-noise estimate and the measured fluctuations in the DCR tracks the difference between the measured DCR and the “True DCR.”

Fig. 3(b) shows the count rate obtained when the LED illuminates the GPD pixel. This measured ICR includes contributions from the room temperature dark counts and after pulsing. The figure also shows the True ICR that is adjusted for the after-pulse contributions with the same correction factor used for the DCR at a given bias. Similar to the dark signal plotted in Fig. 3(a), the amount of the after pulsing increases with the applied bias, however, the increase seems to start at a slightly lower bias voltage. Again, the increase in the count-rate

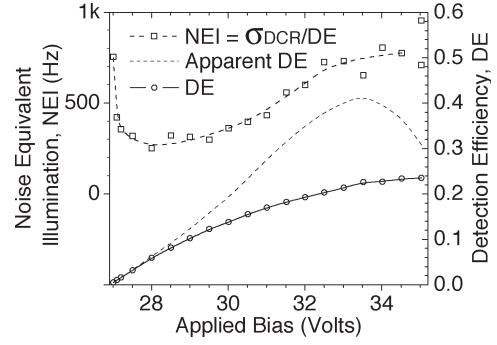


Fig. 4. Plot of the NEI, the DE, and the apparent DE, as a function of the applied bias. The left axis provides the scale for the NEI, which ranges from 300–800 Hz, and the right axis provides a scale for the DE, which varies from zero to 22%.

fluctuations, relative to the Schottky-noise estimation, tracks the increase in the after-pulsing signal.

At applied voltages greater than 34 V, the passive quenching of the GPD pixels with the 80-k $\Omega$  resistor breaks down. This produces a saturation effect, where the measured count rates decrease with increasing bias, as seen in Fig. 3 above 34 V.

#### IV. DISCUSSION

Using the data in Fig. 3, we calculate the DE, the “apparent” DE, and the NEI as a function of the applied bias, as plotted in Fig. 4.

The NEI represents the amount of incident illumination needed, in Hz, to equal the DCR fluctuations, i.e., the noise, in the GPD pixel. It represents a figure of merit for low-light level applications and it does not depend on an illumination signal. Equation (1) defines the NEI plotted in Fig. 4

$$NEI = \frac{\sigma_{DCR}(1-s \text{ integration})}{DE} \quad (1)$$

where  $\sigma_{DCR}$  represents the fluctuation in the DCR measured using a 1-s sampling time, and DE denotes the detection efficiency. This definition of the NEI refers to a “per pixel” quantity, however, it is easily related to the conventional “per area” NEI.

The “apparent” DE represents the DE calculated without correcting for the contribution of the after pulses to the measured count rates and it tracks the true DE at low-bias voltages, where the after pulsing is negligible. The DE increases with the applied bias and, for this pixel, reaches a maximum of  $\sim 22\%$  for 632-nm photons. The QE refers to the efficiency for detecting a photosignal when the pixel is operated as a normal photodiode. It is approximately 60%, and  $\sim 30\%$  of the incident light is reflected from the surface of the pixel. To examine the noise characteristics of our CMOS GPD pixels, we selected a pixel with a large DCR. The same pixel on other chips from the same fabrication run exhibit a room temperature DCR of  $\sim 600$  Hz at the applied bias that produces a DCR of 5 kHz in the pixel used in this paper.

The Geiger detection-efficiency performance is comparable to previous devices reported in the literature. The DCR of the pixel selected for in this paper, however, is generally higher

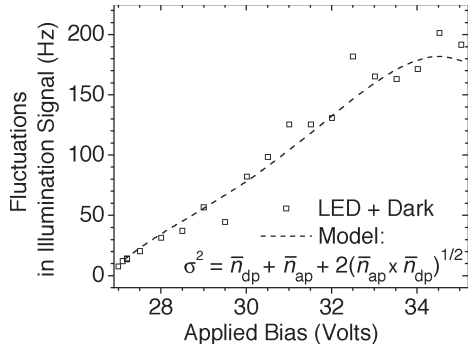


Fig. 5. Comparison of the fluctuations in the ICR to the fluctuations predicted assuming a correlation between the Geiger pulses, from both thermal and optical sources, and the after pulses.

than that previously reported. For example, Cova *et al.* report DCRs of  $\sim 190$  Hz [6] and  $\sim 670$  Hz [9] at room temperature, and 5 V above breakdown, when translated to an equivalent  $30\text{-}\mu\text{m}$  diameter size. Kindt and Van Zeijl show DCRs of  $\sim 2$  kHz under similar conditions. In fact, our earlier, non-CMOS devices exhibit DCRs of  $\sim 200$  Hz at 3 V above breakdown [7]. The DCR of the  $60\text{-}\mu\text{m}$  diameter pixels is a factor of 4 times larger than that of the  $30\text{-}\mu\text{m}$  diameter pixels.

Fig. 5 compares the fluctuations in the ICR, plotted in Fig. 3 (b), to the anticipated fluctuations based on an estimate assuming correlated fluctuations between the after pulses and the detection photons.

Equation (2) describes the total expected count-rate fluctuations based on the sum of two correlated variables, such as the Geiger pulses from the detected photons and the after pulses

$$\sigma^2 = \bar{n}_{dp} + \bar{n}_{ap} + 2\sqrt{\bar{n}_{dp} \cdot \bar{n}_{ap}} \quad (2)$$

where  $\sigma$  represents the total count-rate fluctuations, the “dp” subscript stands for “detected photons,” the “ap” subscript stands for “after pulses,” and the  $\bar{n}$  represents the average count rate of dp, or ap. The sum of the detected photons and the after pulses yields the total count rate. The total count-rate fluctuations described by (2) contains the fluctuations of the detected photons, the fluctuations of the after pulses, and a correlation term. Fig. 5 illustrates the good agreement between the measured fluctuations and the estimate based on (2). The estimate based on (2) assumes that the detected photons and after pulses are perfectly correlated Poisson processes. Equation (2) produces a reasonable estimate of the signal fluctuations when the after pulsing probability is  $< 0.5$ . When the after pulsing probability increases, however, a deviation from (2) is expected because the after pulsing obeys a geometric probability distribution function. An increase in the after-pulsing probability might be expected for devices fabricated in type III–V materials, which contain more traps, or when the GPD pixel is actively quenched, which improves the detection of after pulses created by short-lived traps.

We use (2) to estimate the signal-to-noise ratio (SNR) for the LED signal, where the DCR is subtracted from the ICR and this difference is divided by the fluctuations, because it produces smoother curves, as illustrated by the plot in Fig. 6.

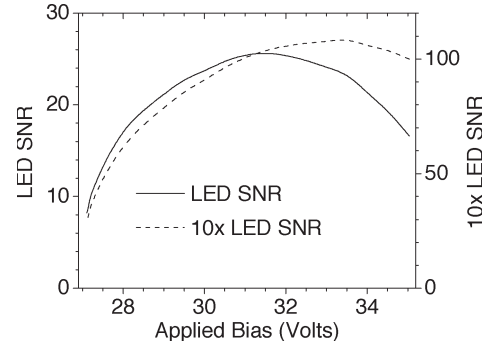


Fig. 6. Plot of the SNR for the LED signal, and the expected SNR for the LED with a factor-of-10 increase in the illumination intensity.

The BOV refers to the applied bias that optimizes the SNR. The minimum in the NEI, of  $\sim 300$  Hz at 28 V, represents the BOV for very small signals. Fig. 6 shows that the BOV shifts from 31 V for a 10 kHz incident-photon signal denoted LED SNR, to 33 V for an extrapolated signal of 100 kHz. The BOV and the maximum SNR depend on the magnitude of the incident signal, and the amount of fluctuations introduced by after pulsing.

To first-order, the increase in the room-temperature DCR tracks the increase in the DE. Higher order effects include an increase in the DCR caused by the expansion of the depletion width in the GPD pixel. The after pulses generally originate from the liberation of the trapped charge. Kindt and Van Zeijl have modeled the amount of the after pulsing in a GPD pixel [8]. Their model explains the bias-voltage dependence of the after-pulsing probability as the increased current in the Geiger pulse populates more trap sites. Rochas and coworker have also examined the after pulsing in their single photon avalanche photodiode pixels (SPADs) [12]. They observe an after-pulsing probability of 7.5% at an excess bias of 5 V.

On the time scales associated with the passive quenching of the GPD pixel, greater than  $1\ \mu\text{s}$ , the transient heating of the depletion region by the Geiger pulse may provide an additional consideration in the source of after pulses. In essence, the DCR may increase immediately after a Geiger pulse. We estimate that the increase in the temperature caused by a Geiger pulse is  $\sim 0.8\ ^\circ\text{C}$  at 1 V above the BV, assuming a 10-pF total pixel capacitance, a 10-nm depletion width, and using a heat capacity of  $20\ \text{J}/(\text{K} \cdot \text{mol})$ . At 3.3 V above breakdown, the estimated transient increase in the temperature is  $\sim 0.8\ ^\circ\text{C}$ , however, this simplistic estimate neglects the transport of heat from the depletion region to the surrounding substrate.

## V. CONCLUSION

In this paper, we have shown that the after pulsing in our GPD pixel introduces additional count-rate fluctuations, which are accurately described by (2). This expression contains a term for the correlation between the Geiger pulses from the detected photons and the after pulses. The BOVs depends on the intensity of light, and for the selected pixel ranges from 31–33 V for incident illumination intensities of 10 and

100 kHz, respectively. We have also shown that the noise added by the after pulsing in the DCR shifts the best room-temperature operating voltage of the selected GPD pixel down to 28 V for very low-light signals.

#### ACKNOWLEDGMENT

The authors would like to thank the reviewers for their input.

#### REFERENCES

- [1] N. Hijazi, I. Krisch, and B. J. Hosticka, "Wireless power and data transmission system for a micro implantable intraocular vision aid," *Biomed. Tech. (Berl.)*, vol. 47, pp. 174–175, 2002.
- [2] E. R. Fossum, "CMOS image sensors: Electronic camera-on-a-chip," *IEEE Trans. Electron Devices*, vol. 44, no. 10, pp. 1689–1698, Oct. 1997.
- [3] G. Meynants, B. Dierickx, and D. Scheffer, "CMOS active pixel image sensor with CCD performance," in *Proc. SPIE—Int. Society Optl Eng*, 1998, vol. 3410, pp. 68–76.
- [4] J. Janesick, "Charge coupled CMOS and hybrid detector arrays," *Proc. SPIE*, vol. 5167, pp. 1–18, 2003.
- [5] H. Dautet, P. Deschamps, B. Dion, A. D. MacGregor, D. MacSween, R. J. McIntyre, C. Trotter, and P. P. Webb, "Photon counting techniques with silicon avalanche photodiodes," *Appl. Opt.*, vol. 32, no. 21, pp. 3894–3900, Jul. 1993.
- [6] S. Cova, M. Ghioni, A. Lacaita, C. Samori, and F. Zappa, "Avalanche photodiodes and quenching circuits for single-photon detection," *Appl. Opt.*, vol. 35, no. 12, p. 1956, Apr. 1996.
- [7] S. Vasile, P. Gothoskar, R. Farrell, and D. Sdrulla, "Photon detection with high gain avalanche photodiode arrays," *IEEE Trans. Nucl. Sci.*, vol. 45, no. 3, pp. 720–723, Jun. 1998.
- [8] W. J. Kindt and H. W. Van Zeijl, "Modelling and fabrication of Geiger mode avalanche photodiodes," *IEEE Trans. Nucl. Sci.*, vol. 45, no. 3, pp. 715–719, Jun. 1998.
- [9] E. Sciacca, A. C. Giudice, D. Sanfilippo, F. Zappa, S. Lombardo, R. Consentino, C. Di Franco, M. Ghioni, G. Fallica, G. Bonanno, S. Cova, and E. Rimini, "Silicon planar technology for single-photon optical detectors," *IEEE Trans. Electron Devices*, vol. 50, no. 4, pp. 918–925, Apr. 2003.
- [10] B. Aull, A. H. Loomis, D. J. Young, R. M. Heinrichs, B. J. Felton, P. J. Daniels, and D. J. Landers, "Geiger mode avalanche photodiodes for three dimensional imaging," *Linc. Lab. J.*, vol. 13, no. 2, pp. 335–350, 2002.
- [11] J. C. Jackson, D. Phelan, A. P. Morrison, R. M. Redfern, and A. Mathewson, "Toward integrated single-photon-counting microarrays," *Opt. Eng.*, vol. 42, no. 1, pp. 112–118, Jan. 2003.
- [12] P. A. Besse, B. Furrer, M. Gani, N. Gisin, R. S. Popovic, G. Ribordy, and A. Rochas, "Single photon detector fabricated in a complementary metal-oxide-semiconductor high-voltage technology," *Rev. Sci. Instrum.*, vol. 74, no. 7, pp. 3263–3270, Jul. 2003.



**William G. Lawrence** was born in New Orleans, LA, in 1963. He received the B.S. degree in chemistry from Louisiana State University, Baton Rouge, and the Ph.D. degree from the University of California, Irvine, in 1985 and 1992, respectively. His Ph.D. research focused on the use of optical probes to study condensed-phase reaction dynamics and included work on the development of solid-state excimer lasers.

He received postdoctoral fellowships to work at the Free University Berlin and the synchrotron radiation source Berliner Elektronenspeicherring-Gesellschaft für Synchrotronstrahlung (BESSY), Berlin, Germany. In 1993 he was a Postdoctoral Researcher at Emory University, Atlanta, GA, where he worked on energy transfer processes in the chemical oxygen iodine laser (COIL) and on the spectroscopy and dynamics of small radical–rare gas complexes. In 1997, he began a position as a Principal Scientist at Physical Sciences Inc., North Andover, MA, where he worked on infrared hyperspectral imaging systems and the development of a multispectral light detection and ranging (LIDAR) receiver. In 2001 he began working for Shipley Company Limited-Liability Corporation (LLC) on the development of 157-nm photoresist materials. He was the Shipley Corporate Assignee to the Interuniversity Microelectronics Center (IMEC), Leuven, Belgium, where he worked for 18 months. While at IMEC, he started a program to look at the molecular dynamics of line edge roughness in chemically amplified photoresist. Currently, he is a Senior Scientist at Radiation Monitoring Devices, Watertown, MA. The work is directed towards the development of CMOS Geiger mode photodetectors and the development of instruments based on APD detectors.



**Frank L. Augustine** (S'78–M'81) received the B.S., M.S., and Ph.D. degrees from Purdue University, West Lafayette, IN, in 1976, 1978, and 1981, respectively.

From 1981 to 1984, he worked for Hewlett-Packard Company, Ft. Collins, CO, doing advanced photolithography development. From 1984 to 1993, he was with Hughes Aircraft Company, Carlsbad, CA, developing processes and front-end application-specified integrated circuits (ASICs) for a variety of cryogenically operated infrared detectors. Since

1993, he has been self-employed as an independent IC designer, specializing in front-end ASICs for radiation, charged particle, visible and infrared detection systems.



**James F. Christian** (M'05) was born in Baltimore, MD, in 1962. He received the B.S. degree in biology and chemistry from Loyola College, MD, and the Ph.D. degree in physical chemistry from the State University of New York at Stonybrook, studying Ion-C<sub>60</sub> collisions with a triple sector guided ion beam instrument, in 1980 and 1992, respectively.

After working at a pharmaceutical company in MD, between 1992 and 1994, he worked as a Postdoctoral Researcher at the Atomic and Molecular Physics Institute (AMOLF) in Amsterdam, The Netherlands, where he studied the dynamics of electron wavepackets in atomic Rubidium. He also worked as a Postdoctoral Research Associate in the Physics Department at Northeastern University, Boston, MA, from 1994 to 1998, where he examined active-site interactions in heme proteins using resonance-enhanced Raman spectroscopy. In September of 1998, he joined Radiation Monitoring Devices, Inc. (RMD), Watertown, MA, as a Staff Scientist, where he worked on APD sensor development. Since October, 2003, he has served as the Group Leader for the Instrument Research and Development (IRD) group at RMD. The IRD group develops radiation sensors and imagers for both high-energy photons, such as X-rays and gamma rays, as well as optical photons, using a variety of detector technologies, including silicon APD and CMOS Geiger photodiode (GPD) devices.

Dr. Christian is currently a member of the American Physical Society and the American Chemical Society.



**Christopher J. Stapels** (M'05) was born in Mt. Clemens, MI, in 1976. He received the B.S. degree in physics and mathematics from Alma College, Alma, MI, and the Ph.D. degree in nuclear physics, from Oregon State University, Corvallis, for his dissertation involving nuclear spectroscopy of nuclei in the transition region from spherical to deformed shapes in 1998 and 2004, respectively.

He participated in the National Science Foundation Research Experiences for Undergraduates (NSF-REU) research program in South Bend, IN, in

1997, working with early radioactive beams. He joined Radiation Monitoring Devices in Watertown, MA, as a Staff Scientist in November 2004. His research interest include design and characterization of CMOS-based avalanche photodiodes (APDs) for use in applications such as scintillator readout and charged-particle tracking.